JOURNAL OF CATALYSIS 61, 299–304 (1980)

Electron-Stimulated and Thermal Desorption Studies on Palladium

I. Oxygen

G. M. BLIZNAKOV AND M. P. KISKINOVA

Institute of General and Inorganic Chemistry, Bulgarian Academy of Sciences, 1040 Sofia, Bulgaria

Received October 10, 1977; revised June 4, 1979

Chemisorption of oxygen on a Pd ribbon has been studied by means of thermal and electron-stimulated desorption mass spectrometry. The results of combined thermal desorption (TD) and electron-stimulated desorption (ESD) experiments indicated the existence of two adsorption states, the more tightly bound one being responsible for the ESD signal. After resolving the desorption curves into two single desorption traces, the desorption energies of the two states were derived. An attempt was made to explain the observed dependence of oxygen coverage and ESD current intensity on adsorption temperature.

INTRODUCTION

Investigation of the adsorption of oxygen on metal surfaces is the first stage in revealing the mechanism of catalytic oxidation processes. The results of investigations (*1–6*) on the oxygen–palladium system indicate dissociative oxygen adsorption. More detailed studies of oxygen adsorption on single-crystal Pd samples have been carried out by the LEED method (*1–4*). The different single-crystal planes (especially the (111) and (100) planes) have been found to possess similar properties with respect to oxygen adsorption. The results of Conrad *et al.* (*4*) are indicative of considerable dissolution of adsorbed oxygen during thermal desorption (TD) when the subsurface region is free of bulk oxygen. TD studies on polycrystalline samples (*5, 6*) have shown the desorption energy, E_d, to be 55 kcal/mol, i.e., within the interval of desorption energies determined on different single-crystal planes.

The purpose of the present work was to study oxygen adsorption on a Pd ribbon using the combination of electron-stimulated and thermal desorption techniques. The appliction of both methods is useful in obtaining information on the adsorption states of the Pd surface.

EXPERIMENTAL

All experiments were performed in a stainless-steel ultrahigh-vacuum chamber pumped both by a 100 liter/sec ion pump and a liquid nitrogen-cooled titanium sublimation pump (base pressure $\sim 10^{-10}$ Torr). The system was equipped with a quadrupole mass spectrometer (QMS) having a deviator for ions (RIBER). The ion source of the QMS was supplemented with a simple electron gun and three-grid electron optics for ESD. The potentials were chosen so as to prevent ions from the gas phase from reaching the detector. Thus the QMS worked in two regimes: (1) for TD and residual gas detection with the ion source filament switched on; (2) for ESD with the electron gun cathode switched on. The polycrystalline palladium ribbon (30 × 1 × 0.02 mm) of 99.999% purity was mounted on a manipulator and could be placed in front of the Ar bombardment gun and the ionizer of the QMS.

The sample was resistively heated. The temperature control was realized using a Pt–PtRh 10% thermocouple, spot welded to the back side of the sample. The signal from the thermocouple controlled a transistor linear programmed heater which ensured a heating rate in the range from 0.5 to

0021-9517/80/020299-06$02.00/0

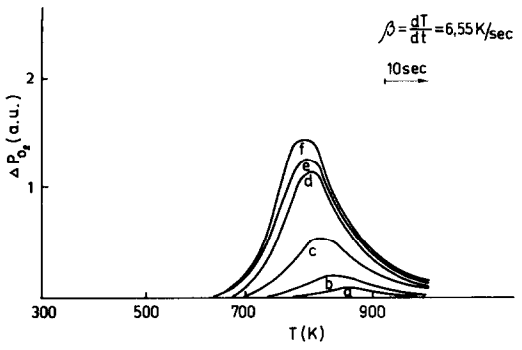

FIG. 1. TD curves of O_2 from Pd at various oxygen exposures at 300°K: (a) 3×10^{-7}; (b) 4.5×10^{-7}; (c) 9×10^{-7}; (d) 1.8×10^{-6}; (e) 3.6×10^{-6}; (f) 5.4×10^{-6} Torr × sec.

200°K/sec. To eliminate the influence of the heating current on the thermocouple reading, two thin (0.08-mm) Pt wires were welded to the sample on either side of the Pt–PtRh as described by Tracy and Palmberg (*7*).

The sample was cleaned by a prolonged Ar bombardment and heated, followed by heating in oxygen at 1000°K. As was shown elsewhere (*8*), a similar cleaning procedure gives surfaces free of C and S. Heating in oxygen ($P_{O_2} \sim 1 \times 10^{-7}$ Torr) was repeated between the experimental cycles because the concentration of carbon on the surface considerably increased during electron-stimulated desorption (ESD) experiments. As is shown by Conrad *et al.* (*4*), a similar procedure eliminated the influence of oxygen dissolution on the TD spectra.

The experiments were carried out at an oxygen partial pressure of 8×10^{-8} Torr. Under these conditions, the partial pressure of CO from the background was below 4%. Thus the oxygen adsorption runs were carried out at CO impurity concentrations which were sufficiently low and could not affect the experimental results described below.

RESULTS

Thermal Desorption Studies

Figure 1 shows the series of TD curves obtained at different oxygen exposures at 300°K. With increasing coverage, the maxima of the TD curves are shifted toward lower temperature. Previous investigations (*1–6*) showed that oxygen is adsorbed in the form of atoms and desorbed as molecules, which presupposes second-order desorption kinetics. A slight broadening of the TD traces was observed at higher temperatures. This may be due to a more strongly bound adsorption state or to side effects during TD, such as the temperature gradient along the sample, desorption from the sample ends, etc. However, these effects could be neglected because the ESD optics system between the sample and the QMS was fitted to ensure the detection of desorption flux only from the central part of the sample.

2. Combined Thermal and Electron-Stimulated Desorption

On electron bombardment of the Pd surface covered with oxygen, desorption of O^+ ions was recorded. Figure 2 shows the change in the intensity of O^+ current, I_{O^+}, and in the oxygen coverage, θ (determined from the TD spectra), as functions of oxygen exposure at $T = 300$°K. It is obvious that I_{O^+} reaches a maximum value at coverages θ ranging from 0 to 0.2; after a very slight decrease, the I_{O^+} value remains constant and is not affected by the further increase of θ. It should be noted that the maxi-

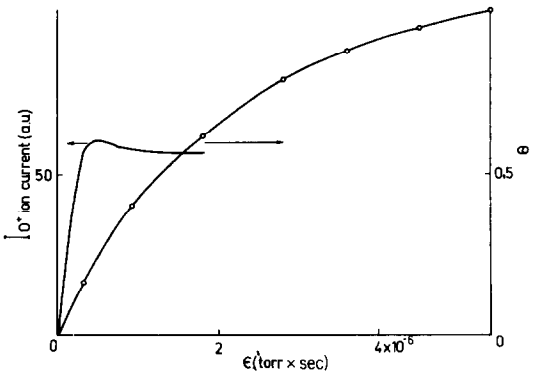

FIG. 2. Intensity of O^+ ion current, I_{O^+}, and oxygen coverage, θ, as a function of the exposure, ϵ, at 300°K.

mum coverage θ_{max} under our experimental conditions was assumed to be 1.

In combined ESD and TD experiments, a change in the ion current during TD was recorded (Fig. 3). It can be seen that a decrease of I_{O^+} began at temperatures at which part (1/2) of the oxygen coverage had already been desorbed. The behavior of the ESD signal during adsorption and thermal desorption suggested the existence of a second adsorption state active with respect to ESD and representing small part of the total oxygen coverage. By differentiation of the trace $I_{O^+}(T)$ in Fig. 3 the shape of the desorption curve corresponding to the more strongly bound adsorption state was determined. The desorption energy obtained from the temperature of the peak maximum using Redhead's relationship (*11*) for a second-order desorption process was 57 kcal/mol.

Assuming that the TD curves in Fig. 1 represent desorption from two independent surface states, the following experiments were run for separating these two states. The Pd ribbon saturated with adsorbed oxygen was first heated to a temperature corresponding roughly to the desorption of the lower temperature state. After that the sample was recooled to room temperature *in vacuo* and subsequently reflashed to complete desorption. Thus, the higher temperature adsorption state, representing less

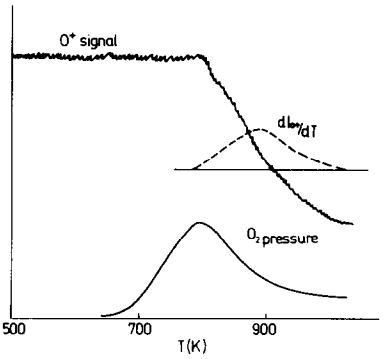

FIG. 3. TD curve and change in the I_{O^+} recorded during heating of Pd, saturated with oxygen ($\theta = \theta_{max} = 1$). The dashed line presents the desorption curve obtained by differentiation of the $I_{O^+}(T)$ plot.

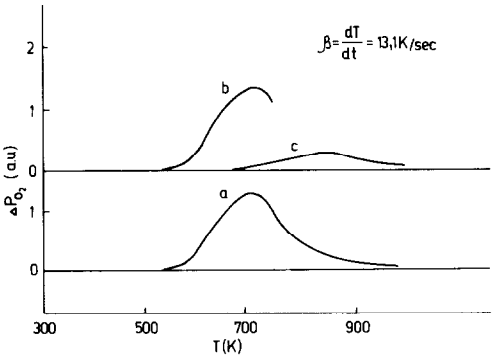

FIG. 4. TD curves: (a) normal TD curve, recorded on heating up to 1000°K; (b) TD curve obtained on heating to 750°K; (c) TD curve recorded on reheating until completion of desorption. The initial oxygen coverage is $\theta_{max} = 1$.

than 0.1 of the θ_{max}, was recorded (Fig. 4). The E_d for this state was found to be 56 kcal/mol. Within the experimental error of temperature detection which is ∓ 10°K, the above E_d value almost coincides with the value determined from the curve in Fig. 3. The study of the lower temperature state which, as is shown above, represents the main part of the oxygen coverage, was performed assuming dependence of E_d and ν on θ. Thus the TD curves can be described by an equation of the kind:

$$-\frac{d\theta}{dt} = \nu(\theta)\,\theta^2 \exp[-E_d(\theta)/RT] \quad (1)$$

where the desorption energy E_d and the frequency factor ν are independent functions of the coverage θ.

In order to determine $E_d(\theta)$ and $\nu(\theta)$, a full line-shape analysis of the TD traces was made by the method described in detail by Bauer *et al.* (*9*, *10*). The initial values obtained for E_d and ν remain constant for θ lower than 0.2. The observed weak dependence of E_d and ν on oxygen coverage for $\theta > 0.2$ can be interpreted in terms of a lateral interaction model (*12*, *13*) by assuming a rather weak repulsive interaction between the adsorbed species in comparison with the attractive forces between them and the solid surface (see Fig. 5). The reliability of the initial E_d values, found by the above

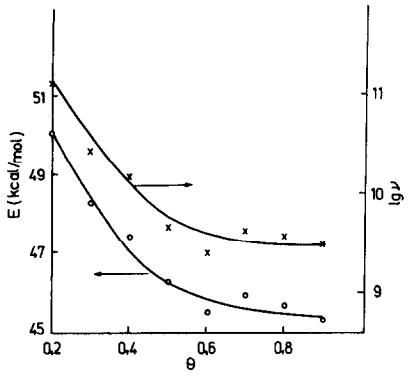

FIG. 5. Energy of desorption, E_d, and frequency factor, ν, as a function of oxygen coverage for $\theta > 0.2$.

method, was checked using the simple relationship proposed by Redhead (*11*):

$$\ln \frac{T_p \theta}{\beta} = \frac{E_d}{RT_p} + \ln \frac{E_d}{\nu AR} \qquad (2)$$

where T_p is the temperature of the peak maximum. E_d can be determined without assuming a value of the frequency factor by varying the rate of heating β and plotting $\ln(T_p\theta/\beta)$ against $1/T_p$. Since this method requires E_d to be independent of θ, we used TD curves recorded at coverages lower than 0.2. From the slope of the plot, shown in Fig. 6, E_d was found to be 51 kcal/mol. Within the limits of error (±2 kcal/mol), this value almost coincides with the initial E_d value shown in Fig. 5.

From the area below the TD curves, the oxygen desorption amount could be evaluated and plotted as a function of exposure. On the basis of this plot we determined the sticking coefficient, s, as a function of oxygen coverage, shown in Fig. 7. The absolute value of the initial sticking coefficient, s_0, was found to be 0.35.

A series of TD and ESD experiments on oxygen adsorption at higher temperatures was carried out. In order to eliminate adsorbate–adsorbate interactions the appropriate exposure was chosen to ensure a coverage below 0.2 at 300°K. Figure 8 shows a change in I_{O^+} and in θ with adsorption temperature T_a. It is evident that within the temperature range 300–400°K θ increases, after which, with further increase of T_a, it decreases. The plot $I_{O^+}(T_a)$ has a similar shape, but the maximum value of the O^+ signal is attained at T_a above 560°K.

DISCUSSION

The dependences observed in the combined TD and ESD studies suggest a two-state model for oxygen adsorption. As is evident from Fig. 2, I_{O^+} is proportional to coverage for θ less than 0.2. Since drastic changes in the ESD cross-section at such low coverages are almost impossible, we assume the existence of adsorption centers, characterized by a higher desorption energy, which represent a very small part of the whole surface sites. Since the probability of ESD strongly depends on the exact adsorbate configuration, it is only the oxygen adsorbed at these sites which gives a measurable ESD signal. The effect of surface irregularities on adsorption characteristics was studied in detail by Somorjai *et al.* (*14, 15*). As is shown by Hagen *et al.* (*15*) the TD spectra of oxygen from stepped Ir surfaces exhibit the same two peaks which were observed on the polycrystalline samples (*16*). The lower temperature desorption peak is the same as is found on the equilibrium (111) Ir plane, while the higher temperature one is due to the desorption

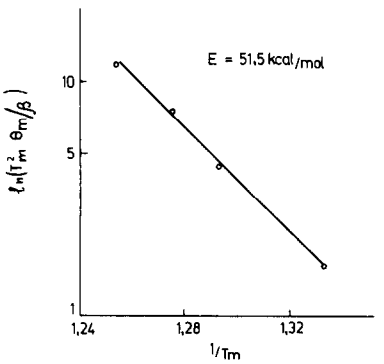

FIG. 6. $\ln T_m^2\theta_m/\beta$ as a function of $1/T_m$ for series of experiments in which heating rate, β, is varied. T_m is the temperature of the TD peak maximum, which under our experimental conditions (high pumping speed) is equal to T_p.

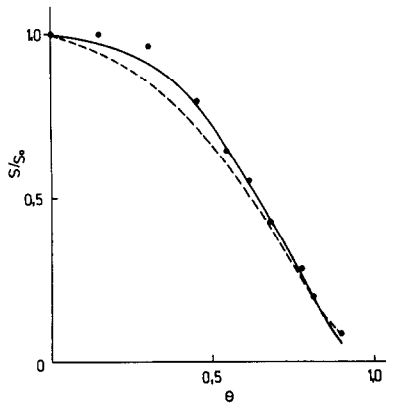

FIG. 7. Theoretical fit to the normalized sticking coefficient, s/s_0, vs. θ. The solid line corresponds to Eq. (3''), and the dashed line to Eq. (3') at k and $k' = 0.2$. The points correspond to the experimentally obtained values.

from the steps. Thus the more strongly bound oxygen adsorption state suggested in the present study could be ascribed to the oxygen adsorbed on surface irregularities. Another possible explanation may be associated with the existence of a "surface oxide" phase (see Conrad *et al.* (*4*)) whose formation is favored by the high-temperature treatment with oxygen during the cleaning procedure. As is shown by Conrad *et al.* (*4*), this phase is stable at temperatures up to 1000°K and may influence the neighboring adsorption sites.

The dependence of θ and I_{O^+} on adsorption temperature shown in Fig. 8 can be explained on the basis of a correlation between the sticking coefficient s and the adsorption temperature T_a. According to the model of condensation given by Ehrlich (*17*) and generalized by Tamm and Schmidt (*18*) and by Kisliuk (*19*), chemisorption passes through an intermediate state and the sticking coefficient is determined by two competing processes; namely, chemisorption and desorption of the intermediate state.

This model can be used in our case of dissociative adsorption since the latter undoubtedly occurs via a precursor state according to the scheme:

$$O_2^g \underset{k_d^*}{\overset{s^*}{\rightleftarrows}} O_2^* \xrightarrow{k_c G(\theta)} 2O_a$$

where s^* is the sticking coefficient of the precursor state, k_d^* and k_c are the rate constants of desorption and conversion into the tightly bound chemisorption state, O_a, of the precursor form O_2^*, and $G(\theta)$ is the probability of finding a suitable vacant chemisorption site which, in the case of two-site adsorption, is $(1 - \theta)^2$.

On the basis of the model proposed by Kisliuk (*19*), Clavenna and Schmidt (*20*) gave the following equation for the sticking coefficient:

$$s = \frac{S^*}{1 + \{P_d(1 - \theta) + P'_d\theta\}/P_c G(\theta)} \quad (3)$$

where P_d and P'_d are the probabilities of desorption at an empty and a filled neighboring center, respectively, and P_c is the probability of chemisorption from the precursor state O_2^*.

This equation has two limiting cases:

(1) The desorption from the precursor state is independent of the occupation of the neighboring sites, i.e., $P_d = P'_d$. Then Eq. (3) can be written as:

$$s = \frac{s_0(1 + k)}{1 + k/G(\theta)} \quad (3')$$

where s_0 is the sticking coefficient of chemisorption $= s^*/(1 + k)$.

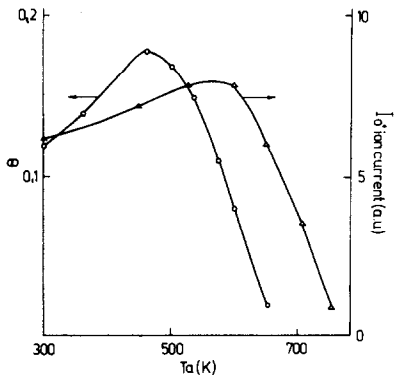

FIG. 8. I_{O^+} and θ as a function of the adsorption temperature, T_a, at an oxygen exposure $\epsilon = 9 \times 10^{-7}$ Torr × sec.

(2) The probability of desorption when the neighboring sites are occupied, P'_d, is much higher than P_d, i.e., $P'_d \gg P_d$. Then Eq. (3) can be written as:

$$s = \frac{s_0}{1 + k'\theta/G(\theta)} \qquad (3'')$$

where $k' = P'_d/P_c$.

Using expressions (3') and (3''), we plotted the theoretical curves of s/s_0 as functions of θ. The best agreement with the experimental data was shown by the model for which $P'_d \gg P_d$ and $k' = 0.2$ (see Fig. 7). Thus, in our case it can be assumed that the sticking coefficient is described by Eq. (3'') where only the coefficient k' is temperature dependent. The latter is defined by the equation:

$$k' = P'_d/P_c \sim 1/[\exp(E^*_d - E_{diff})/RT].$$

Here, E^*_d is the activation energy of desorption of the precursor state and E_{diff} is the activation energy of migration to the chemisorption center. If the precursor state at lower temperatures is relatively immobile, E_{diff} will have a high value which may exceed E^*_d. Then s will increase with increasing temperature. If the precursor state becomes mobile above a certain temperature, and E_{diff} decreases to such an extent that it becomes lower than E^*_d, s will decrease with increase of temperature.

This model satisfactorily explains the experimental data in Fig. 8 if the two binding states are independent of each other, as was assumed in the interpretation of the combined TD and ESD data.

The dependence of θ and I_{O^+} on T_a could also be explained by the possibility of dissolution of oxygen into the bulk of Pd at higher temperatures, reported in detail in the literature (*4, 21, 22*). Hence the behavior of the curves in Fig. 8 can be interpreted assuming that the lower temperature state penetrates into the bulk more easily, i.e., at lower temperatures. The results obtained in the present paper reveal a rather complex behavior of the Pd–O_2 system. Further studies are necessary to give explicit explanation of the observed effects.

ACKNOWLEDGMENT

Thanks are due to Dr. L. Surnev for valuable discussions and help with experiments.

REFERENCES

1. Ertl, G., and Rau, P., *Surf. Sci.* **15,** 443 (1973).
2. Ertl, G., and Koch, J., *Z. Phys. Chem. N.F.* **69,** 323 (1970).
3. Ertl, G., and Koch, J., II Int. Symp. Ads. Des. Phen., 1972.
4. Conrad, H., Ertl, G., Kuppers, J., and Latta, E. E., *Surf. Sci.* **65,** 245 (1977).
5. Ertl, G., and Koch, J., Proc. 5th Int. Cong. Catalysis (Florida, 1972), p. 969. North Holland/American Elsevier, Amsterdam/New York, 1973.
6. Bliznakov, G., Marinova, Ts., and Kiskinova, M., *Compt. R. Bulg. Acad. Sci.* **1,** 93 (1976).
7. Tracy, J. C., and Palmberg, P. W., *J. Chem. Phys.* **51,** 4852 (1969).
8. Surnev, L., Bliznakov, G., and Kiskinova, M., Proc. IVth Int. Conf. Catalysis, Varna, 1979 (in press).
9. Bauer, E., Poppa, H., and Todd, G., *J. Appl. Phys.* **45,** 237 (1974).
10. Engel, T., Bauer, E., and Niehus, H., *Surf. Sci.* **52,** 237 (1975).
11. Redhead, P. A., *Vacuum* **12,** 203 (1962).
12. Adams, D. L., *Surf. Sci.* **42,** 12 (1974).
13. King, D. A., *Surf. Sci.* **47,** 384 (1975).
14. Somorjai, G. A., Joyner, R. W., and Lang, B., *Proc. R. Soc. London A* **331,** 335 (1972).
15. Hagen, D. I., Nieuwenhuys, B. I., Rovida, G., and Somorjai, G., *Surf. Sci.* **56,** 2 (1976).
16. Ageev, V. N., and Ionov, N. I., *Z. Tekn. Fiz.* **41,** 2196 (1973).
17. Ehrlich, G., *J. Phys. Chem.* **59,** 473 (1955).
18. Tamm, P. W., and Schmidt, L. D., *J. Chem. Phys.* **51,** 5352 (1969); **52,** 1150 (1970).
19. Kisliuk, P., *J. Phys. Chem. Solids* **5,** 78 (1958); **3,** 95 (1957).
20. Clavenna, L. R., and Schmidt, L. D., *Surf. Sci.* **22,** 365 (1970).
21. Palazov, A., *J. Catal.* **36,** 251 (1975).
22. Close, J. S., and White, J. M., *J. Catal.* **36,** 185 (1975).